

Noise-like pulses generated at high harmonics in a partially-mode-locked km-long Raman fiber laser

A. Boucon · B. Barviau · J. Fatome · C. Finot ·
T. Sylvestre · M.W. Lee · P. Grellu · G. Millot

Received: 24 January 2011 / Revised version: 30 July 2011 / Published online: 7 January 2012
© Springer-Verlag 2011

Abstract We present a 5-km-long Raman fiber laser that delivers pulses at high harmonics of the fundamental cavity repetition rate, up to 1 GHz. The observed nanosecond pulses that propagate in an anomalous dispersion regime possess a complex noise-like structure with a coherence time of around 1 picosecond.

1 Introduction

All-fiber lasers have been intensively investigated due to their scalable cavity design and alignment-free operation, leading to their use in various domains from telecommunications to spectroscopy. The amplification process has mostly been achieved by using rare-earth-doped fibers which limit the range of emission wavelengths to existing bands of fluorescence. This limitation almost disappears by using the Raman amplification, which has already been used in continuous-wave (cw) fiber lasers for the past two decades, in particular for the specific physical mechanisms which occur in such long fiber cavity [1]. For short-pulse operation, the use of Raman amplification is more recent, with the first demonstration of a passively mode-locked Raman fiber laser five years ago in a figure-of-eight cavity [2]. One year later, Randoux et al. presented a Raman fiber ring laser operating

on the fourth-order forward Raman Stokes component [3]. These two configurations used a normal cavity dispersion scheme that promotes single pulse operation at the fundamental cavity repetition rate.

Harmonic mode-locking, where the laser operates at a multiple of its fundamental frequency, is one possible solution to increase the repetition rate of fiber lasers. Although active mode-locking has allowed to generate harmonics up to 165,000 [4], this technique is limited by the bandwidth of electronic devices, in addition to a bulky design with a complex setup. Since the first report in 1993 of passive harmonic mode-locking in a soliton Er/Yb-codoped fiber laser [5], numerous studies have followed [6–9]. In particular, self-induced modulational instability (MI) process generates high-order harmonics in Er-doped fiber laser [10, 11] and 160-GHz pulses in a Raman fiber laser, by using a fiber Bragg grating [12, 13]. Considering high-harmonics achievements with passive mode-locking using nonlinear polarization evolution, an Er-doped double-clad fiber laser operating on the 322nd harmonic has recently been demonstrated [14].

In this paper, we report on a novel Raman fiber laser configuration that generates train of pulses at very high harmonics (up to 24,480th, 1-GHz repetition rate) through the combined use of nonlinear polarization evolution and Raman gain in a km-long cavity. The generated pulses are in fact noise-like incoherent pulses made up of a complex ultrashort subpulse structure [15–17]. A classical time distribution reconstruction has been used in order to indicate the plausible pulse structure from ps to ns time scales. We further demonstrated the tunability of repetition rate from 100 MHz to 1 GHz by controlling the intracavity polarization. This work contributes to a further understanding of the complex time and pulsed dynamics of Raman fiber laser.

A. Boucon (✉) · B. Barviau · J. Fatome · C. Finot · P. Grellu ·
G. Millot
Laboratoire Interdisciplinaire Carnot de Bourgogne, UMR 5209
CNRS, Université de Bourgogne, 21078 Dijon, France
e-mail: anne.boucon@draka.com

T. Sylvestre · M.W. Lee
Département d'Optique P. M. Duffieux, Institut FEMTO-ST,
Université de Franche-Comté, CNRS UMR 6174, 25030
Besançon, France

2 Experimental setup

The experimental setup is sketched in Fig. 1. The pump laser is a 1480-nm cw Raman fiber laser, which couples from 1.3 to 3 Watts into the single-mode fiber ring cavity through a wavelength-division multiplexer (WDM). The Raman gain medium is a 5-km dispersion-shifted fiber (DSF) whose zero-dispersion wavelength is located at 1549.6 nm and has a chromatic dispersion of $\beta_2 \approx -3.93$ ps²/km at 1581.5 nm.

The DSF is enclosed between two polarization controllers. In principle, for specific orientations of the polarization controllers, the polarization-sensitive losses induced by the intracavity polarizer enable passive mode-locking, thanks to the nonlinear polarization evolution that takes place during propagation in the long fiber cavity [18–20]. The polarization-insensitive optical isolator ensures that only backward Raman-scattered field components can be recirculated in the cavity. We have measured the integrated Raman gain of the DSF for the first-order Stokes backward-

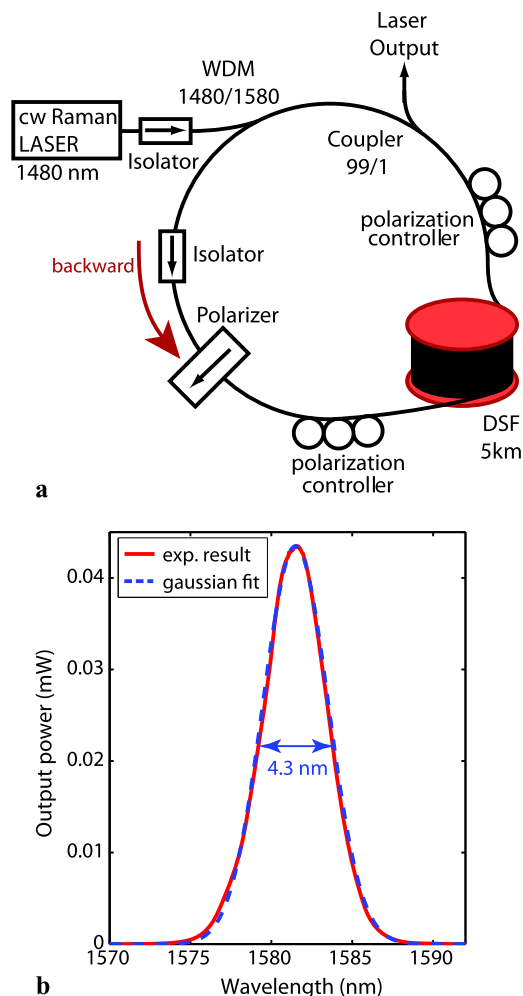


Fig. 1 (a) Raman fiber laser experimental setup. (b) Optical spectrum at the laser output

propagating component. This pump-power-dependent gain increases from 10.8 dB to 26.56 dB, when the pumping power is raised from 1.3 to 3 Watts. Finally, we have inserted a 1% output coupler to extract the laser signal and measured its optical and RF spectra as well as the temporal evolution of the optical intensity with optical and electrical spectrum analyzer and a 12-GHz real-time oscilloscope. Once the all-fibered cavity configuration is set, the regime of operation depends on the pumping power and the orientations of the polarization controllers. The lasing threshold for the first-order backward-propagating Raman component is 1 W. With an appropriate setting of the polarization controllers, pulsed operation at either the fundamental cavity repetition rate or its harmonics can be achieved at a pumping power of 1.3 W.

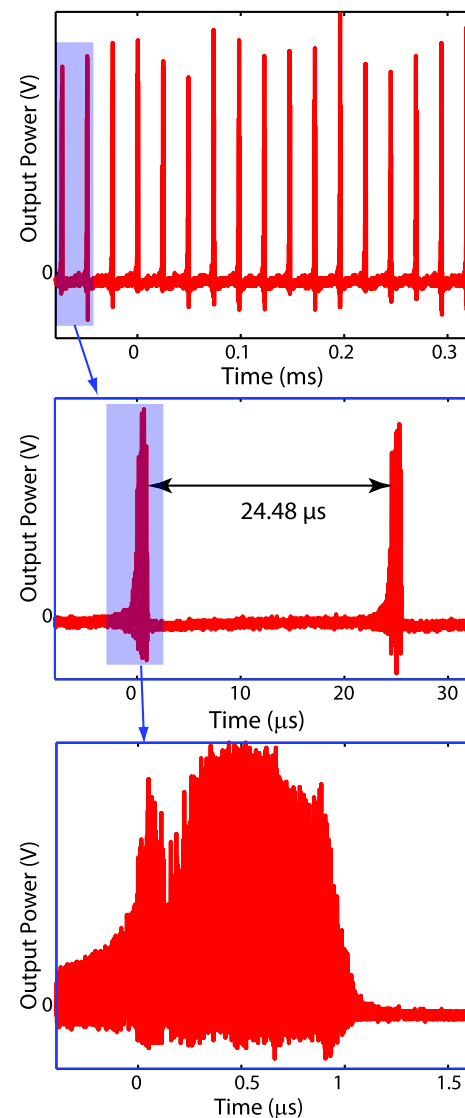


Fig. 2 Oscilloscope output signal at the fundamental frequency

3 Experimental results

Adjusting the polarization controllers, we obtain a train of pulses separated by 24.48 μs , which corresponds to the fundamental cavity repetition rate of 40.85 kHz, as displayed in Fig. 2. As shown in Fig. 1b, the lasing wavelength is around 1581.5 nm and lies inside the anomalous dispersion regime of the fiber. This spectrum is well fitted by a 4.3-nm Gaussian function, and the bandwidth is compatible with the emission of approximately 850-fs Fourier-transform pulses.

However, the temporal magnification of the pulses in Fig. 2 reveals a substructure, which lets us assume multiple pulsing and pulse bunching as commonly found in an anomalous dispersion regime under high pumping power [6, 21–23]. The substructure in Fig. 2 matches to a microsecond-long irregular bunch of pulses. Adjusting further the orientations of the polarization controllers and increasing the pumping power, we observe that the substructure splits into a high-harmonic pulsed regime. Indeed, adjusting the polarization controllers results in altering the effective nonlinear cavity transmission, which directly affects the interac-

tion between pulses and the total intracavity energy [8, 22, 24].

In our case, depending on the orientations of polarization controllers, we have observed stable pulsations at the following high harmonics of the cavity fundamental repetition rate: 100, 140, 260, 330, 410, 580, 800, 850, 950 MHz, and 1 GHz. Two RF spectra of harmonic pulse regimes are presented in Figs. 3a and b. In Fig. 3a, the repetition rate is 1 GHz (corresponding to about 24,480 times of the fundamental repetition rate of the ring cavity). We have analyzed in details the 140-MHz-repetition rate, which is very stable, with a low amount of supermode noise (with a dynamic of 40 dB) as shown in the inset of Fig. 3b.

Figure 4 shows pulse train (a) and autocorrelation trace (b) of the output signal at 140 MHz. The output intensity recorded in Fig. 4a is made with 2.5-ns-long pulses, showing again a possible noisy substructure. The autocorrelation trace displays a 1.4 ps-wide coherence peak on a background level of 0.4, thus demonstrating the weak temporal coherence of the laser [15]. So we can legitimately assume that these 2.5-ns-long pulse structures represent irregular bunches of shorter pulses, in a way similar to the ps-

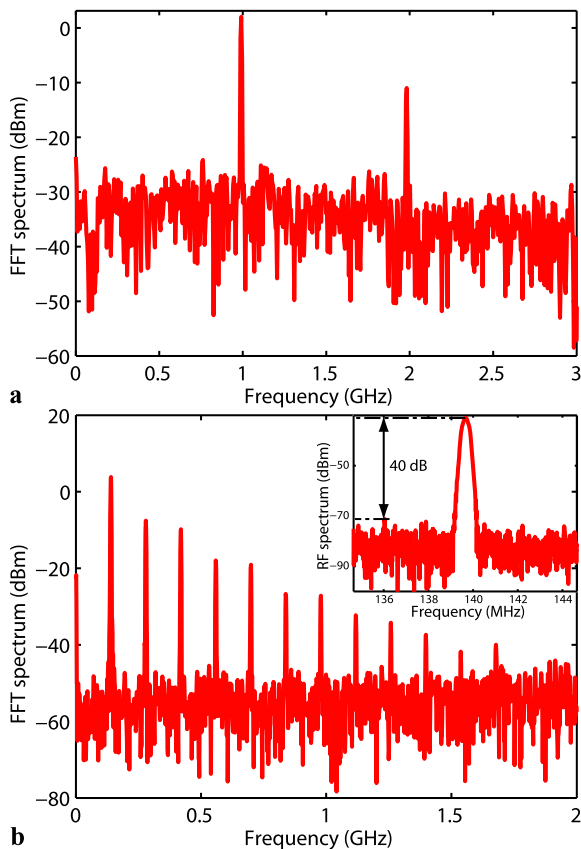


Fig. 3 FFT spectrum of the output signal for two different harmonic repetition rates of (a) 1 GHz for an input power of 3 W and a mean output signal of 7.5 dB m and (b) 140 MHz for input power of 2.9 W and a mean output signal of 8 dB m. The inset is an RF spectrum recorded from an RF analyzer and shows a supermode suppression of 40 dB

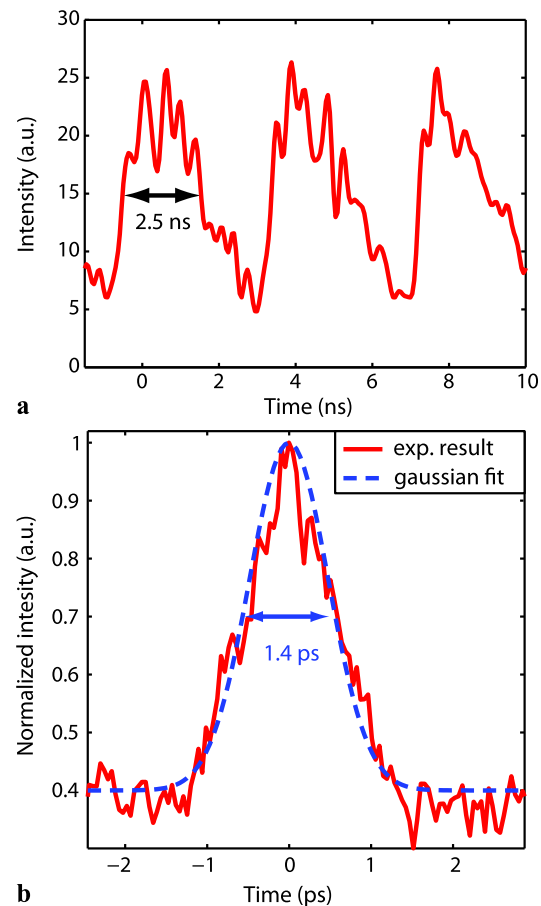


Fig. 4 (a) Pulse train observed from oscilloscope with a 6-GHz band-pass electronic. (b) Autocorrelation trace of the output signal. Pulse repetition rate: 140 MHz

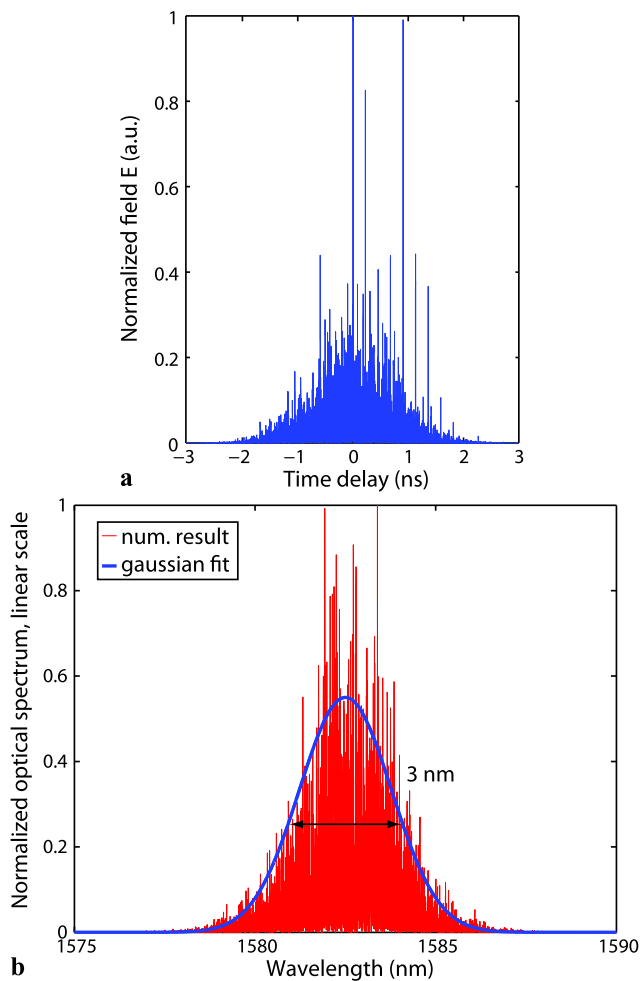


Fig. 5 (a) Optical field modeled by a sum of sech, with random time delay between them and random phase. (b) Optical spectrum associated with this optical field

time scale intensity fluctuations recently observed in long continuous-wave Raman fiber lasers [25, 26]. This might indicate that the physical mechanisms that are at play in the noise-like pulses in our laser could also result from multiple nonlinear interactions between the cavity modes through the interplay of four-wave mixing and cavity dispersion [27, 28].

In order to strengthen this hypothesis, we have numerically constructed an optical field as the sum of picosecond pulses. Then we have multiplied each of the spectral component by a random phase noise $e^{i\phi}$, where ϕ is a random number belonging to the interval $[0, 2\pi \times \alpha]$, and α is a positive real number, inferior to unity. We have multiplied the corresponding temporal signal with a 2.5-ns Gaussian-function. In the phase noise expression, α determines the degree of correlation between the spectral modes: if $\alpha = 0$, the spectral modes are totally correlated, and the autocorrelation trace presents no pedestal. If $\alpha = 1$, the spectral modes are

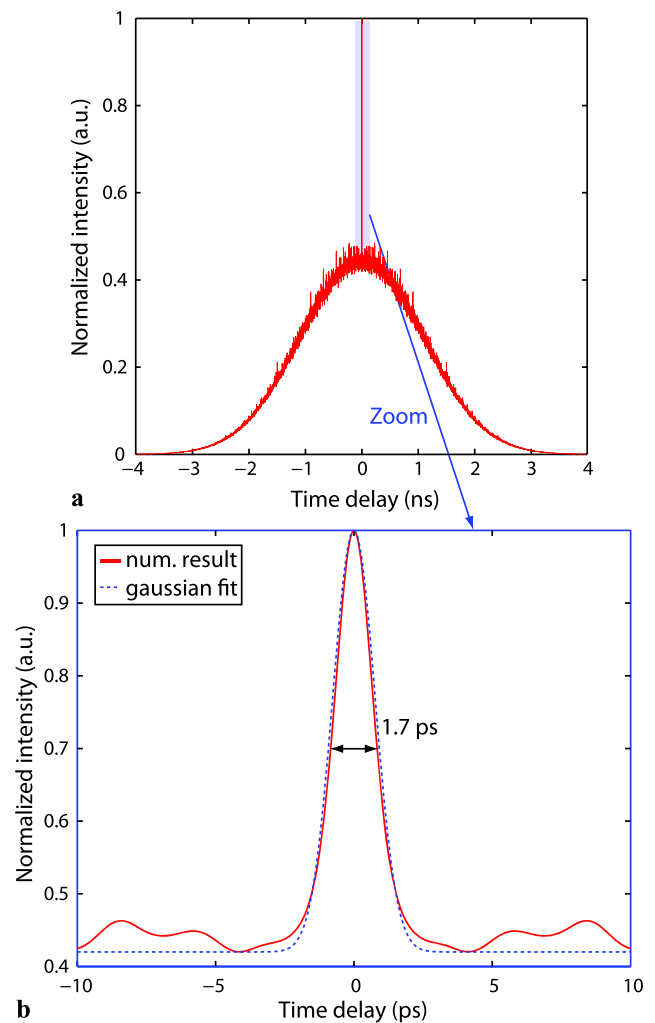


Fig. 6 (a) Autocorrelation function associated with this optical field. (b) Zoom of the central autocorrelation function shows a full width at half maximum of 1.7 ps

totally decorrelated, and the autocorrelation trace presents a pedestal of 50%.

In this reconstruction, we have used $\alpha = 0.828$ in order to obtain a pedestal of 40%, in concordance with the experimental results. The hypothetical optical field envelope is represented in Fig. 5a, and the associated optical spectrum in Fig. 5b has been fitted with a 3-nm Gaussian function, a bandwidth similar to the experimental one. Correspondingly, Fig. 6a shows the calculated autocorrelation trace, with a magnification in Fig. 6b in a good agreement with the experimental autocorrelation trace.

4 Conclusions

We have experimentally demonstrated a high-harmonic partially mode-locked Raman fiber laser, operating on the backward first-Stokes component. The pulses are generated with

a repetition rate up to 24400 times the fundamental cavity repetition rate and are associated with noise-like substructures as was observed in Ref. [15] for the fundamental cavity rate of an erbium-doped laser. In addition to bringing new results on the relatively unexplored area of mode-locked Raman fiber lasers, we confirm the importance of noise-like pulses among self-organized pulsed dynamics that can arise in long fiber laser cavities. It is also remarkable that noise-like pulse can be manifested with high harmonics.

Acknowledgements We acknowledge P. Suret and S. Randoux from Laboratoire de Physique des Lasers, Atomes et Molécules, UMR-CNRS 8523 in Lille, for productive scientific discussions.

References

1. S.K. Turitsyn, J.D. Ania-Castañón, S.A. Babin, V. Karalekas, P. Harper, D. Churkin, S.I. Kablukov, A.E. El-Taher, E.V. Podivilov, V.K. Mezentsev, *Phys. Rev. Lett.* **103**, 133901 (2009)
2. D.A. Chestnut, J.R. Taylor, *Opt. Lett.* **30**, 2982 (2005)
3. S. Randoux, P. Suret, *Opt. Commun.* **267**, 145 (2006)
4. K.S. Abedin, M. Hyodo, N. Onodera, *Opt. Lett.* **26**, 151 (2001)
5. A.B. Grudinin, D.J. Richardson, D.N. Payne, *Opt. Lett.* **18**, 358 (1993)
6. A.B. Grudinin, S. Gray, *J. Opt. Soc. Am. B* **14**, 144 (1997)
7. S. Zhou, D.G. Ouzounov, F.W. Wise, *Opt. Lett.* **31**, 1041 (2006)
8. Z.X. Zhang, L. Zhan, X.X. Yang, S.Y. Luo, Y.X. Xia, *Laser Phys. Lett.* **4**, 592 (2007)
9. L.M. Zhao, D.Y. Tang, T.H. Cheng, C. Lu, H.Y. Tam, X.Q. Fu, S.C. Wen, *Opt. Quantum Electron.* **40**, 1053 (2008)
10. C.J. S de Matos, D.A. Chestnut, J.R. Taylor, *Opt. Lett.* **27**, 915 (2002)
11. L.M. Zhao, D.Y. Tang, D. Liu, *Appl. Phys. B* **99**, 441 (2010)
12. J. Schröder, S. Coen, F. Vanholsbeeck, T. Sylvestre, *Opt. Lett.* **31**, 3489 (2006)
13. J. Schröder, D. Alasia, T. Sylvestre, S. Coen, *J. Opt. Soc. Am. B* **25**, 1178 (2008)
14. F. Amrani, A. Haboucha, M. Salhi, H. Leblond, A. Komarov, P. Grelu, F. Sanchez, *Opt. Lett.* **34**, 2120 (2009)
15. M. Horowitz, Y. Barad, Y. Silberberg, *Opt. Lett.* **22**, 799 (1997)
16. M.A. Putnam, M.L. Dennis, I.N. Duling III, C.G. Askins, E.J. Friebele, *Opt. Lett.* **23**, 138 (1998)
17. S. Kobtsev, S. Kukarin, S. Smirnov, S. Turitsyn, A. Latkin, *Opt. Express* **17**, 20707 (2009)
18. B. Nikolaus, D. Grischkowsky, A.C. Balant, *Opt. Lett.* **8**, 389 (1983)
19. V.J. Matsas, T.P. Newson, D.J. Richardson, D.N. Payne, *Electron. Lett.* **28**, 2226 (1992)
20. A. Komarov, A. Haboucha, F. Sanchez, *Opt. Lett.* **33**, 2254 (2008)
21. F. Gутty, Ph. Grelu, N. Huot, G. Vienne, G. Millot, *Electron. Lett.* **37**, 745 (2001)
22. S. Chouli, P. Grelu, *Phys. Rev. A* **81**, 63829 (2010)
23. F. Amrani, M. Salhi, H. Leblond, F. Sanchez, *Appl. Phys. B* **99**, 107 (2010)
24. G. Martel, C. Chédot, A. Hideur, Ph. Grelu, *Fiber Integr. Opt.* **27**, 320 (2007)
25. S.A. Babin, D.V. Churkin, A.E. Ismagulov, S.I. Kablukov, E.V. Podivilov, *J. Opt. Soc. Am. B* **8**, 1729 (2007)
26. S. Randoux, N. Dalloz, P. Suret, *Opt. Lett.* **6**, 790 (2011)
27. S.A. Babin, V. Karalekas, V.K. Mezentsev, P. Harper, J.D. Ania-Castañón, S.K. Turitsyn, *Phys. Rev. A* **77**, 33803 (2008)
28. J. Schroeder, S. Coen, *Opt. Express* **17**, 16444 (2009)